Sensor and Simulation Notes

Note 452

26 January 2001

Maximizing Total and TEM Mode Power Through an Azimuthal Waveguide Bend Filled with a Graded Dielectric Medium

Michael J. Walker
Carl E. Baum

Air Force Research Laboratory
Directed Energy Directorate

ABSTRACT

This effort examines and attempts to maximize the transmission of a fast rise-time signal through a TEM waveguide with a bend. To maintain the fast rise-time, a graded dielectric medium is used in the waveguide bend, eliminating the dispersion associated with increased pathlength at a larger radius. However, the tradeoff is a power loss due to reflections at the material discontinuities where two straight waveguide segments loaded with constant dielectric medium are attached to the bend. Additionally, some of the power that is transmitted through the bend couples into higher order modes. The centerline reference value of the graded dielectric in the bend can be chosen, based on the bend's curvature and the dielectric value in the adjoining straight segments, to maximize either total power transmitted or TEM mode power transmitted. Matching the centerline value of the bend's dielectric to the adjoining straight segments' dielectric is shown to be a very good "rule of thumb." While not mathematically optimal, it allows more than 99.5% of the maximum power transmission, especially for low curvature bends. This optimal dielectric value is also shown to be independent of the bend's angle.

This work was sponsored in part by the Air Force Office of Scientific Research (AFOSR) and in part by the Air Force Research Laboratory, Directed Energy Directorate.

1. INTRODUCTION

This effort examines a TEM waveguide with a bend and attempts to maximize its transmission of fast rise-time signals. To maintain the rise time, a graded dielectric medium is used in the waveguide bend to eliminate dispersion. Like a straight TEM waveguide, a waveguide bend filled with a continuously graded dielectric medium can support a pure azimuthal TEM mode [1,2]. However, the material discontinuities where two straight waveguide segments are attached to the bend will cause some of the transmitted power to couple into higher order modes and cause additional power losses due to material discontinuity reflections at the boundaries. The dielectric material in the bend can be optimized for any curvature and straight segment dielectric value to minimize reflections and maximize power transmission independent of the bend angle. The geometry of the problem analyzed is shown in Figure 1.

Although higher order modes are known to exist in the bend and in the transmitted region, they do not need to be rigorously modeled because we are primarily interested in the early-time, high-frequency limit of the waveguide's performance. From this perspective, all that is necessary are expressions for the total transmitted power and the fraction of that power still in the TEM mode. By not modeling the higher-order modes, the transmission of energy across the second boundary cannot exactly account for any variations of incidence angle. However, the high-frequency components responsible for the early-time shape of the signal, while dispersed, are still expected to follow the bend and arrive at the second boundary at near normal incidence. Thus, the normal transmission coefficient is assumed sufficiently accurate to describe the coupling of leading-edge energy across the second boundary. Appendix A briefly addresses the low-frequency requirement for matching the guide impedances between regions.

Several additional assumptions were also made about the problem being investigated. The goal was to maximize the power through each boundary while maintaining the fast rise time of the leading edge. Therefore, a "steady-state" transmission coefficient for the entire bend was not calculated. A "steady-state" analysis would require tracking and summing the total transmitted power contributions due to multiple reflections propagating forward and backward down the length of the waveguide. While these components do contribute to the total transmitted power, their propagation delay through the waveguide is at least three times the transit time of the leading edge of the signal. Therefore, their contribution of output power is too late to be included in the component of the signal we were trying to maximize. Instead, "instantaneous" coefficients at each boundary were derived, and their product was considered the total transmission coefficient.

It was assumed that the dielectric material in both of the straight waveguide segments was identical. It was also assumed that no dielectric variation in the azimuthal direction or the direction of the rotational axis existed for both the continuously graded bend and the straight segments. The material in all the segments was also assumed non-magnetic and lossless. Finally, the walls were assumed to be perfect electric conductors. In Figure 1, the subscript "i" was meant to label "incident" variables. However, since the material parameters in the other straight segment are assumed equal, they are subscripted "i" also. Appendix B briefly addresses the situation when the parameters in the straight segments are not equal. All variables subscripted "ref" are measured with respect to the centerline radius of the bend.

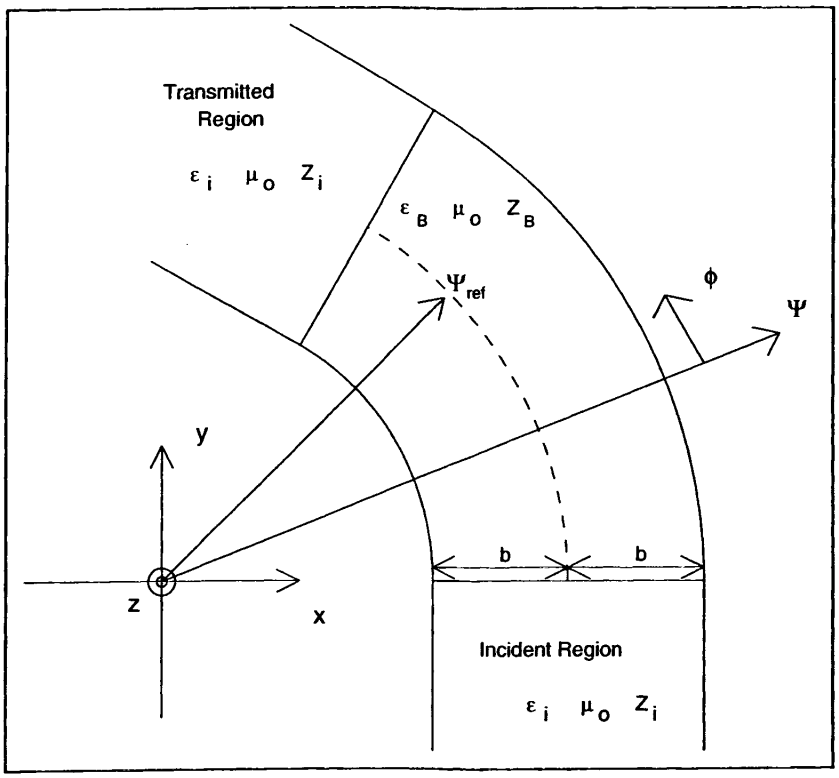

Figure 1: Problem Geometry

This analysis was initially performed on an E-plane waveguide bend, assumed either infinitely long in the 'z' direction or long enough with respect to the width of the waveguide that fringing effects could be ignored. Additional analysis confirmed that the results also apply to an H-plane waveguide bend, assuming either the height was small enough with respect to the width that the fringing effects could be ignored or that magnetic boundary conditions could and had been enforced [3 (Section 4)]. A generalized drawing of the waveguide bend applicable to each case is shown in Figure 2.

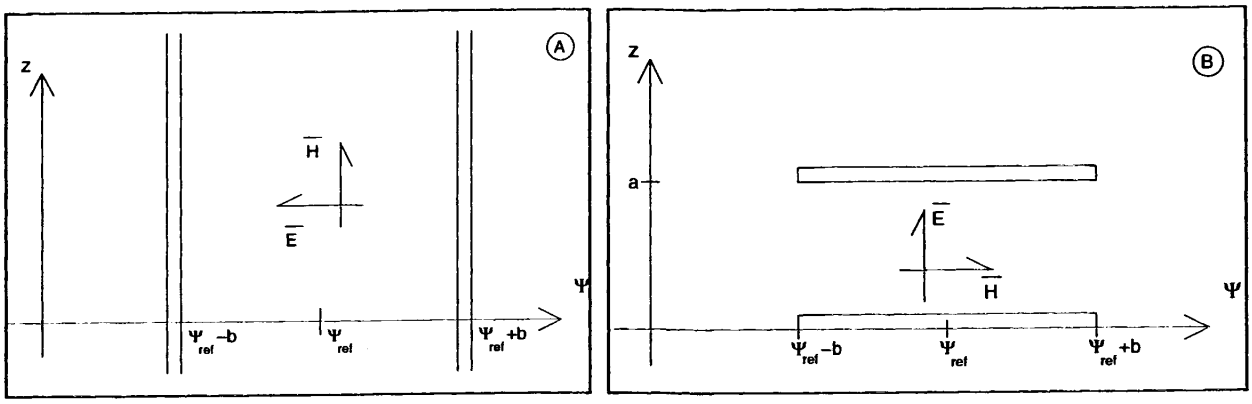

Figure 2: Waveguide Cross-Sections for E-plane (A) and H-Plane (B) Bends

2. DERIVATION

The expression for the graded dielectric in the waveguide bend [1] is

$$\varepsilon_B = \varepsilon_{ref}\left(\frac{\Psi_{ref}}{\Psi}\right)^2. \tag{1}$$

The intrinsic impedance of the dielectric in the waveguide bend [1] is

$$Z_B = \sqrt{\frac{\mu_o}{\varepsilon_B}} = \sqrt{\frac{\mu_o}{\varepsilon_{ref}}}\left(\frac{\Psi}{\Psi_{ref}}\right) = Z_{ref}\left(\frac{\Psi}{\Psi_{ref}}\right) \tag{2}$$

where

$$Z_{ref} = \sqrt{\frac{\mu_o}{\varepsilon_{ref}}}, \tag{3}$$

while the intrinsic impedance in the incident and transmitted regions is

$$Z_i = \sqrt{\frac{\mu_o}{\varepsilon_i}}. \tag{4}$$

2.1. TRANSMITTED ELECTRIC FIELD

When a TEM wave is normally incident on the first boundary, the ratio of the transmitted to the incident electric field is

$$\frac{E_2}{E_1} = \frac{2Z_2}{Z_2 + Z_1} \tag{5}$$

where $Z_1 = Z_i$ and $Z_2 = Z_B$. After substituting Z_i, Z_B, and equation (2), and rearranging terms, the resulting ratio is

$$\frac{E_B}{E_i} = \frac{2\Psi Z_{ref}}{\Psi Z_{ref} + \Psi_{ref} Z_i}. \tag{6}$$

At the second boundary, the transmission ratio is also given by equation (5), however the impedance terms are reversed, $Z_1 = Z_B$ and $Z_2 = Z_i$. After substitution, the resulting ratio is

$$\frac{E_T}{E_B} = \frac{2\Psi_{ref} Z_i}{\Psi Z_{ref} + \Psi_{ref} Z_i}. \tag{7}$$

Multiplying equations (6) and (7) produces the ratio of the transmitted total field strength in the second straight waveguide segment to the incident TEM field in the first straight segment, valid in an early-time sense.

$$\frac{E_T}{E_i} = \frac{4\Psi\Psi_{ref} Z_{ref} Z_i}{(\Psi Z_{ref} + \Psi_{ref} Z_i)^2} \tag{8}$$

Figure 3 shows a variety of possible electric field strength variations across the output waveguide for different values of Z_{ref}/Z_i with a normalized radius, Ψ/Ψ_{ref}, as the independent variable. The center of the waveguide is located at $\Psi/\Psi_{ref} = 1.0$ and extends a distance $\kappa = b/\Psi_{ref}$ in each direction. The portion of the field lines plotted in Figure 3 and falling between the vertical limits $1-\kappa<\Psi/\Psi_{ref}<1+\kappa$ describe the field variation across the waveguide.

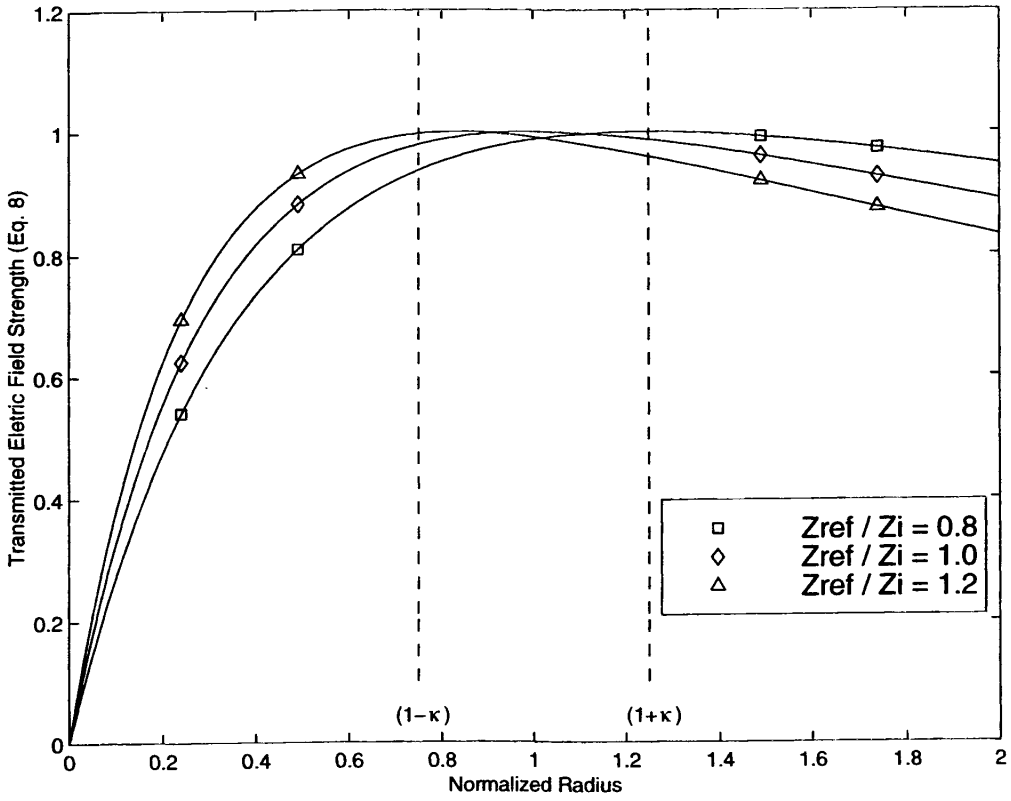

Figure 3: Radial Variation of Transmitted Electric Field Strength (Normalized)

Any TEM mode energy in a straight, parallel plate waveguide must have constant amplitude. Because the amplitudes of the electric field in the bend and in the transmitted region are not uniform, but complicated functions of the radius and impedances, some of the energy must have coupled into higher modes. The magnitude of the total transmitted electric field in the TEM mode can be calculated by integrating the electric field over the aperture of the waveguide [4]. This process is essentially equal to finding the average value of the electric field across the waveguide. The normalized form of this value is calculated below.

$$\frac{(E_T)_{avg}}{E_i} = \frac{1}{2b}\int_{\Psi_{ref}-b}^{\Psi_{ref}+b}\left(\frac{E_T}{E_i}\right)d\Psi = \frac{1}{2b}\int_{\Psi_{ref}-b}^{\Psi_{ref}+b}\frac{4\Psi\Psi_{ref}Z_{ref}Z_i}{(\Psi Z_{ref}+\Psi_{ref}Z_i)^2}d\Psi \tag{9}$$

$$\frac{(E_T)_{avg}}{E_i} = \frac{2\Psi_{ref}Z_i}{bZ_{ref}}\left[\ln(\Psi Z_{ref}+\Psi_{ref}Z_i)+\frac{\Psi_{ref}Z_i}{\Psi Z_{ref}+\Psi_{ref}Z_i}\right]_{\Psi_{ref}-b}^{\Psi_{ref}+b}$$

$$\frac{(E_T)_{avg}}{E_i} = \frac{2\Psi_{ref}Z_i}{bZ_{ref}}\left[\ln\left(\frac{(\Psi_{ref}+b)Z_{ref}+\Psi_{ref}Z_i}{(\Psi_{ref}-b)Z_{ref}+\Psi_{ref}Z_i}\right)+\frac{\Psi_{ref}Z_i}{(\Psi_{ref}+b)Z_{ref}+\Psi_{ref}Z_i}-\frac{\Psi_{ref}Z_i}{(\Psi_{ref}-b)Z_{ref}+\Psi_{ref}Z_i}\right]$$

$$E_{TEM} = \frac{(E_T)_{avg}}{E_i} = \frac{2Z_i}{\kappa Z_{ref}}\left[\ln\left(\frac{(1+\kappa)Z_{ref}+Z_i}{(1-\kappa)Z_{ref}+Z_i}\right)+\frac{Z_i}{(1+\kappa)Z_{ref}+Z_i}-\frac{Z_i}{(1-\kappa)Z_{ref}+Z_i}\right] \tag{10}$$

where $\kappa = b/\Psi_{ref}$.

The amplitude of the normalized TEM mode of the electric field transmitted through the bend, as given in equation (10), is plotted in Figure 4 for several values of Z_{ref}/Z_i. Note that for large curvature bends, there is a 10-15% drop in field strength regardless of impedance. Also, it is actually possible to transmit a stronger TEM electric field through the bend by increasing the value of Z_{ref} compared to Z_i. These observations support the necessity and capability to determine an optimum impedance that maximizes the transmitted TEM power component.

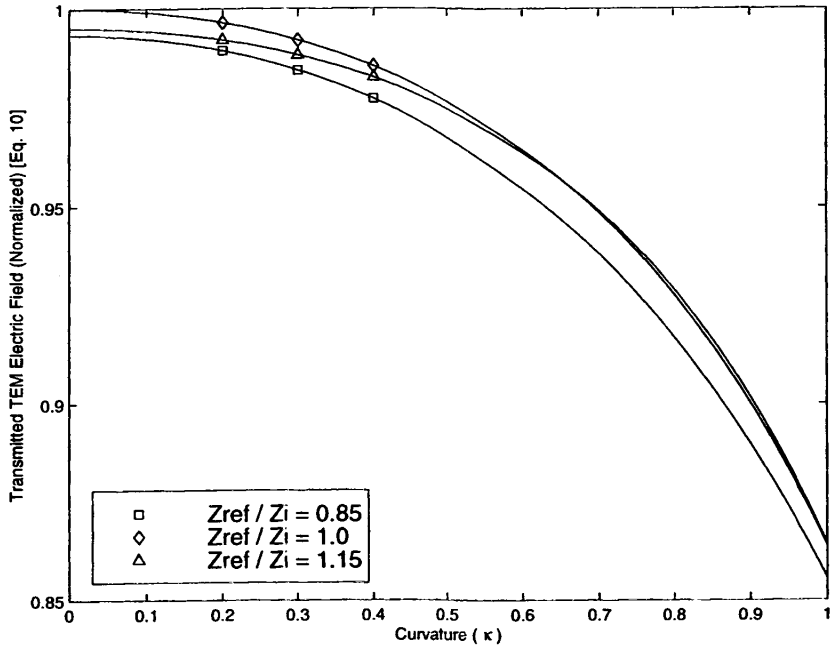

Figure 4: Transmitted TEM Field Strength (Normalized) vs. Curvature

2.2. TRANSMITTED POWER

The power propagating through the waveguide can be calculated by integrating the cross product of the electric and magnetic fields over the cross-sectional area of the waveguide [5]. The input power is

$$P_i = \int_0^a \int_{\Psi_{ref}-b}^{\Psi_{ref}+b} \left|\bar{E}_i \times \bar{H}_i\right| d\Psi\, dz = \frac{E_i^2}{Z_i}(2ab). \tag{11}$$

The total transmitted power is

$$P_{TOT} = \int_0^a \int_{\Psi_{ref}-b}^{\Psi_{ref}+b} \left|\bar{E}_T \times \bar{H}_T\right| d\Psi\, dz = \frac{E_i^2}{Z_i} \int_0^a \int_{\Psi_{ref}-b}^{\Psi_{ref}+b} \left(\frac{E_T}{E_i}\right)^2 d\Psi\, dz \tag{12}$$

$$P_{TOT} = \frac{E_i^2}{Z_i} \int_0^a \int_{\Psi_{ref}-b}^{\Psi_{ref}+b} \left(\frac{4\Psi\Psi_{ref}Z_{ref}Z_i}{(\Psi Z_{ref} + \Psi_{ref}Z_i)^2}\right)^2 d\Psi\, dz$$

$$P_{TOT} = (a)\frac{E_i^2}{Z_i}\left(\frac{16\Psi_{ref}^2 Z_i^2}{Z_{ref}}\right)\left[\frac{-3\Psi^2 Z_{ref}^2 - 3\Psi\Psi_{ref}Z_{ref}Z_i - \Psi_{ref}^2 Z_i^2}{3(\Psi Z_{ref} + \Psi_{ref}Z_i)^3}\right]_{\Psi_{ref}-b}^{\Psi_{ref}+b}$$

$$P_{TOT} = (2ab)\frac{E_i^2}{Z_i}\left(\frac{16Z_i^2 Z_{ref}^2}{3}\right)\left[\frac{3(1-\kappa^2)^2 Z_{ref}^2 + 6(1-\kappa^2)Z_{ref}Z_i + (3+\kappa^2)Z_i^2}{((1-\kappa^2)Z_{ref}^2 + 2Z_{ref}Z_i + Z_i^2)^3}\right]. \tag{13}$$

The transmitted power in the TEM mode is

$$P_{TEM} = \int_0^a \int_{\Psi_{ref}-b}^{\Psi_{ref}+b} \left|\bar{E}_{TEM} \times \bar{H}_{TEM}\right| d\Psi\, dz = \frac{(E_T)_{avg}^2}{Z_i}(2ab). \tag{14}$$

2.3. TRANSMITTED POWER COEFFICIENT DEFINITIONS

Three transmitted power coefficients were defined. First, the total transmission coefficient (T_{TOT}) was defined as the ratio of the total transmitted power (13) to the total input power (11). This quantifies the overall capability of the bend to transmit power in any mode.

$$T_{TOT} = \frac{P_{TOT}}{P_i} = \left(\frac{16Z_i^2 Z_{ref}^2}{3}\right)\left[\frac{3(1-\kappa^2)^2 Z_{ref}^2 + 6(1-\kappa^2)Z_{ref}Z_i + (3+\kappa^2)Z_i^2}{((1-\kappa^2)Z_{ref}^2 + 2Z_{ref}Z_i + Z_i^2)^3}\right] \tag{15}$$

Next, the TEM transmission coefficient (T_{TEM}) was defined as the ratio of the TEM component of the transmitted power (14) to the total input power (11). This quantifies the capability of the bend to transmit TEM mode energy only.

$$T_{TEM} = \frac{P_{TEM}}{P_i} = \left(\frac{(E_T)_{avg}^2 / Z_i}{E_i^2 / Z_i} \right) = \left(\frac{(E_T)_{avg}}{E_i} \right)^2 = E_{TEM}^2 \tag{16}$$

Finally, the power fraction coefficient (T_{PF}) was defined as the ratio of the TEM component of the transmitted power (14) to the total transmitted power (13). This is also the ratio of the other two coefficients. It quantifies the capability of the bend to maintain energy in the TEM mode or to resist coupling energy into higher modes.

$$T_{PF} = \frac{T_{TEM}}{T_{TOT}} = \frac{P_{TEM}/P_i}{P_{TOT}/P_i} = \frac{P_{TEM}}{P_{TOT}} = \frac{E_{TEM}^2}{T_{TOT}} \tag{17}$$

2.4. "MATCHED" TRANSMITTED POWER COEFFICIENT DEFINITIONS

The "matched" case was defined as the situation when the material impedance along the centerline of the bend is set equal to the material impedance of the straight segments ($Z_{ref} = Z_i$). Three "matched" transmitted power coefficients were derived by substituting this value of Z_{ref} into the three transmitted power coefficients above.

$$T_{TOT}^{(m)} = T_{TOT}\big|_{Z_{ref}=Z_i} = \left(\frac{16}{3} \right) \left[\frac{3\kappa^4 - 11\kappa^2 + 12}{\left(4 - \kappa^2\right)^3} \right] \tag{18}$$

$$T_{TEM}^{(m)} = T_{TEM}\big|_{Z_{ref}=Z_i} = \left(\frac{4}{\kappa^2} \right) \left[\ln\left(\frac{2+\kappa}{2-\kappa} \right) - \frac{2\kappa}{4-\kappa^2} \right]^2 \tag{19}$$

$$T_{PF}^{(m)} = T_{PF}\big|_{Z_{ref}=Z_i} = \frac{3\left(4-\kappa^2\right)}{4\kappa^2} \frac{\left[\left(4-\kappa^2\right) \ln\left(\frac{2+\kappa}{2-\kappa} \right) - 2\kappa \right]^2}{\left(3\kappa^4 - 11\kappa^2 + 12\right)} \tag{20}$$

Although Z_{ref} is independent of curvature in the "matched" case, the three "matched" transmitted power coefficients were still dependent on curvature, as shown in Figure 5. Again, it appears there is a lot of room for improving the transmission of power through the bend, especially at high curvature values. No direct effort was made to improve $T_{PF}^{(m)}$ since most of the transmitted power appears to stay in the TEM mode already.

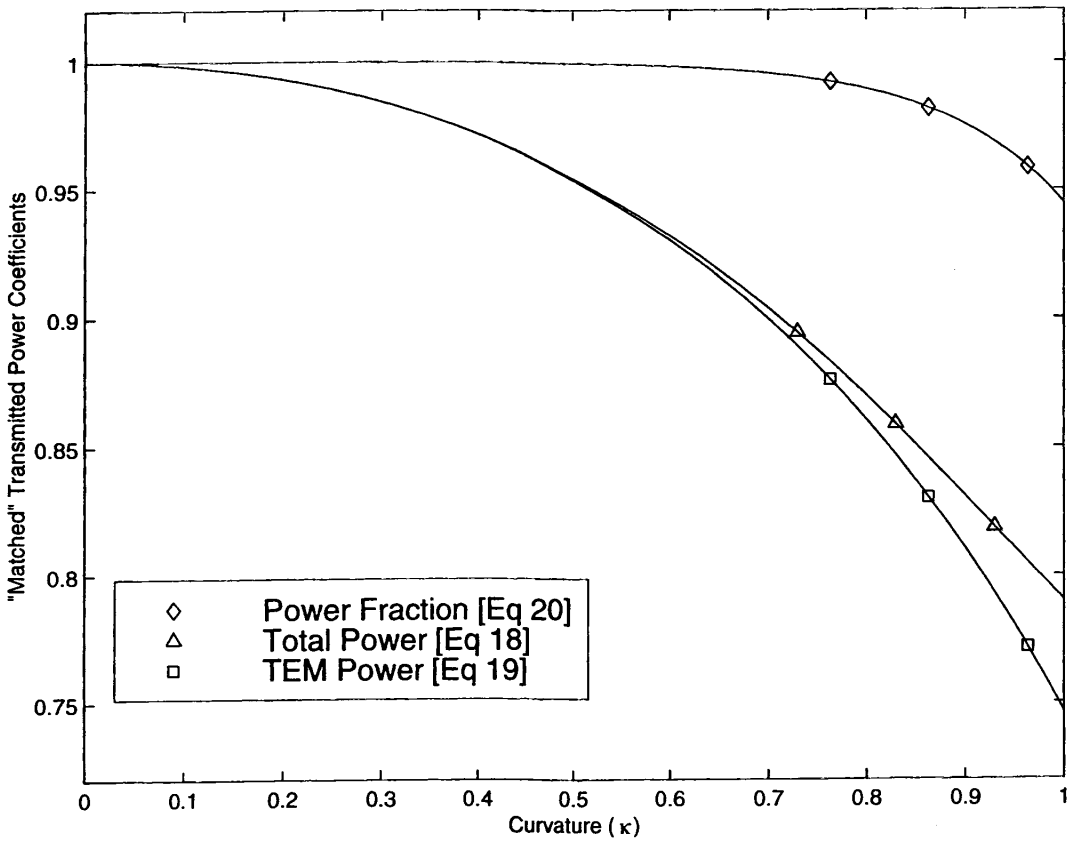

Figure 5: "Matched" Transmitted Power Coefficients vs. Curvature

Most waveguide bends are designed with relatively small values of curvature. Asymptotic expressions for the three "matched" transmission coefficients were derived and are listed below. These approximations are pretty good for curvature values of $\kappa<0.707$ and even better for $\kappa<0.5$. As expected, equations (18)-(20) and their approximations, equations (21)-(23), are all even functions of curvature, allowing the waveguide to have either positive or negative curvature (bend to the left or to the right) with the same results [6].

$$T_{TOT}^{(m)} = T_{TOT}\big|_{Z_{ref}=Z_i} \cong 1 - \frac{\kappa^2}{6} - \frac{\kappa^4}{16} + O\left(\kappa^8\right) \tag{21}$$

$$T_{TEM}^{(m)} = T_{TEM}\big|_{Z_{ref}=Z_i} \cong 1 - \frac{\kappa^2}{6} - \frac{49\kappa^4}{720} - O\left(\kappa^6\right) \tag{22}$$

$$T_{PF}^{(m)} = T_{PF}\big|_{Z_{ref}=Z_i} \cong 1 - \frac{\kappa^4}{180} - O\left(\kappa^6\right) \tag{23}$$

3. OPTIMIZATION

The goal of this effort was to find an expression for the reference impedance along the centerline of the waveguide as a function of curvature that will maximize either the TEM power or the total power through the bend.

3.1. OPTIMIZING TRANSMITTED TEM POWER

The impedance that will maximize the TEM power was found by setting the derivative of E_{TEM} (10) with respect to Z_{ref} equal to zero and solving for Z_{ref}. Unfortunately, the logarithm in (10) caused this to become a transcendental equation. A numerical solution was generated using MatLab® and a plot of the ratio of Z_{ref} to Z_i is shown in Figure 6 in the Results section. An approximate expression for Z_{ref} was also derived numerically using MatLab by fitting a curve to the data in Figure 6. The resulting approximate expression is given in equation (24).

$$Z_{opt}^{(1)} \cong Z_i\left(1+\frac{\kappa^2}{6}+\frac{\kappa^4}{100}+O\left(\kappa^6\right)\right) \qquad \text{for } \kappa < 0.707 \tag{24}$$

3.2. OPTIMIZING TRANSMITTED TOTAL POWER

Another approach for trying to maximize the TEM component of the transmitted power was to maximize the total power transmitted. The idea focussed on the fact that the TEM component is such a large fraction of the total power, the more total power that is transmitted through the bend, the more TEM power will be transmitted also. A closed form expression for the reference impedance in the bend that will maximize the total transmitted power can be found by setting the derivative of T_{TOT} (15) with respect to Z_{ref} equal to zero and solving for Z_{ref}. The derivative is

$$\frac{\partial T}{\partial Z_{ref}} = -\frac{32Z_i^2}{3Z_{ref}} \frac{\left[\begin{array}{c} 3\left(1-\kappa^2\right)^3 Z_{ref}^4 + 6\left(1-\kappa^2\right)^2 Z_{ref}^3 Z_i + 8\kappa^2\left(1-\kappa^2\right) Z_{ref}^2 Z_i^2 \\ +2\left(5\kappa^2-3\right) Z_{ref} Z_i^3 - \left(3+\kappa^2\right) Z_i^4 \end{array}\right]}{\left(\left(1-\kappa^2\right) Z_{ref}^2 + 2Z_{ref} Z_i + Z_i^2\right)^4} = 0.$$

Recognizing that the denominator is never equal to zero, dividing out the constants, and making the substitution

$$X = \left(1-\kappa^2\right)\frac{Z_{ref}}{Z_i}, \tag{25}$$

the expression was simplified to the fourth order polynomial

$$3X^4 + 6X^3 + 8\kappa^2 X^2 + 2\left(5\kappa^2-3\right)X - \left(3+\kappa^2\right)\left(1-\kappa^2\right) = 0. \tag{26}$$

There are four possible solutions to this polynomial. Two solutions are complex conjugates, one is real and always negative, and the last solution is real and always positive. Inverting the substitution (25) and solving for Z_{ref}, only the positive, real solution is valid. That solution is given below. The singularity at $\kappa=1$ can be ignored because equation (1) requires any bend with that curvature to have an infinitely large permittivity at the origin. Thus, neither is possible.

$$Z_{opt}^{(2)} = Z_i \frac{X(\kappa)}{\left(1-\kappa^2\right)} \tag{27}$$

where

$$X(\kappa) = -\frac{1}{6}\left[3 - \sqrt{9+2\kappa R-16\kappa^2} - \sqrt{18-2\kappa R-32\kappa^2 - \frac{18\left(2\kappa^2-3\right)}{\sqrt{9+2\kappa R-16\kappa^2}}}\right], \tag{28}$$

$$R = \sqrt[3]{9\sqrt{Q} - \kappa\left(44\kappa^2-81\right)} - \sqrt[3]{9\sqrt{Q} + \kappa\left(44\kappa^2-81\right)}, \tag{29}$$

and

$$Q = -169\kappa^6 + 537\kappa^4 - 594\kappa^2 + 243\,. \tag{30}$$

Again, recognizing that most waveguide bends are designed with relatively small values of curvature, a single asymptotic expression for equations (27)-(30) was derived and is listed below. This approximation is pretty good for curvature values of $\kappa<0.707$ and even better for $\kappa<0.5$.

$$Z_{opt}^{(2)} \equiv Z_i\left(1+\frac{\kappa^2}{6}-\frac{\kappa^4}{72}+O\left(\kappa^6\right)\right) \qquad \text{for } \kappa < 0.707 \tag{31}$$

3.3. BASELINE RATIO DEFINITIONS

Transmission coefficient data was analyzed for three possible choices of bend impedance; when the impedance is "matched" ($Z_{ref} = Z_i$), when the impedance is optimized for TEM power, and when the impedance is optimized for total power. The results were so similar over so broad a range of values that direct graphical comparison proved difficult. To quantify the benefit of using the two optimized impedances, the "matched" case was used as a baseline for comparison.

The degree of optimization was quantified as the increase in transmitted power using the optimized impedances compared to the amount of transmitted power using the matched impedance. To do this, six additional ratios needed to be defined.

First, the total transmitted power using the two optimized impedances was compared to the total transmitted power using the matched impedance. This is the ratio of equations (15) and (18) after substituting either (24) or (27) into (15).

$$R_{TOT}^{(1)} = \frac{P_{TOT}\left(Z_{ref} = Z_{opt}^{(1)}\right)}{P_{TOT}\left(Z_{ref} = Z_i\right)} = \frac{T_{TOT}\left(Z_{opt}^{(1)}\right)}{T_{TOT}^{(m)}} \tag{32}$$

$$R_{TOT}^{(2)} = \frac{P_{TOT}\left(Z_{ref} = Z_{opt}^{(2)}\right)}{P_{TOT}\left(Z_{ref} = Z_i\right)} = \frac{T_{TOT}\left(Z_{opt}^{(2)}\right)}{T_{TOT}^{(m)}} \tag{33}$$

Next, the TEM component of the transmitted power using the two optimized impedances was compared to the TEM component of the transmitted power using the matched impedance. This is the ratio of equations (16) and (19) after substituting either (24) or (27) into (16).

$$R_{TEM}^{(1)} = \frac{P_{TEM}\left(Z_{ref} = Z_{opt}^{(1)}\right)}{P_{TEM}\left(Z_{ref} = Z_i\right)} = \frac{T_{TEM}\left(Z_{opt}^{(1)}\right)}{T_{TEM}^{(m)}} \tag{34}$$

$$R_{TEM}^{(2)} = \frac{P_{TEM}\left(Z_{ref} = Z_{opt}^{(2)}\right)}{P_{TEM}\left(Z_{ref} = Z_i\right)} = \frac{T_{TEM}\left(Z_{opt}^{(2)}\right)}{T_{TEM}^{(m)}} \tag{35}$$

Last, the TEM power fraction of the transmitted power using the optimized impedances was compared to the TEM power fraction of the transmitted power using the matched impedance. This is the ratio of equations (17) and (20) after substituting either (24) or (27) into (17).

$$R_{PF}^{(1)} = \frac{P_{TEM}\left(Z_{ref} = Z_{opt}^{(1)}\right) / P_{TOT}\left(Z_{ref} = Z_{opt}^{(1)}\right)}{P_{TEM}\left(Z_{ref} = Z_i\right) / P_{TOT}\left(Z_{ref} = Z_i\right)} = \frac{T_{PF}\left(Z_{opt}^{(1)}\right)}{T_{PF}^{(m)}} = \frac{R_{TEM}^{(1)}}{R_{TOT}^{(1)}} \tag{36}$$

$$R_{PF}^{(2)} = \frac{P_{TEM}\left(Z_{ref} = Z_{opt}^{(2)}\right) / P_{TOT}\left(Z_{ref} = Z_{opt}^{(2)}\right)}{P_{TEM}\left(Z_{ref} = Z_i\right) / P_{TOT}\left(Z_{ref} = Z_i\right)} = \frac{T_{PF}\left(Z_{opt}^{(2)}\right)}{T_{PF}^{(m)}} = \frac{R_{TEM}^{(2)}}{R_{TOT}^{(2)}} \tag{37}$$

4. RESULTS

The impedance along the centerline of the waveguide bend was optimized to transmit either the maximum amount of TEM power or the maximum total power through the bend. A plot of both of these impedances as a function of curvature is shown below in Figure 6, with the optimized impedance values normalized to the impedance in the straight waveguide segments.

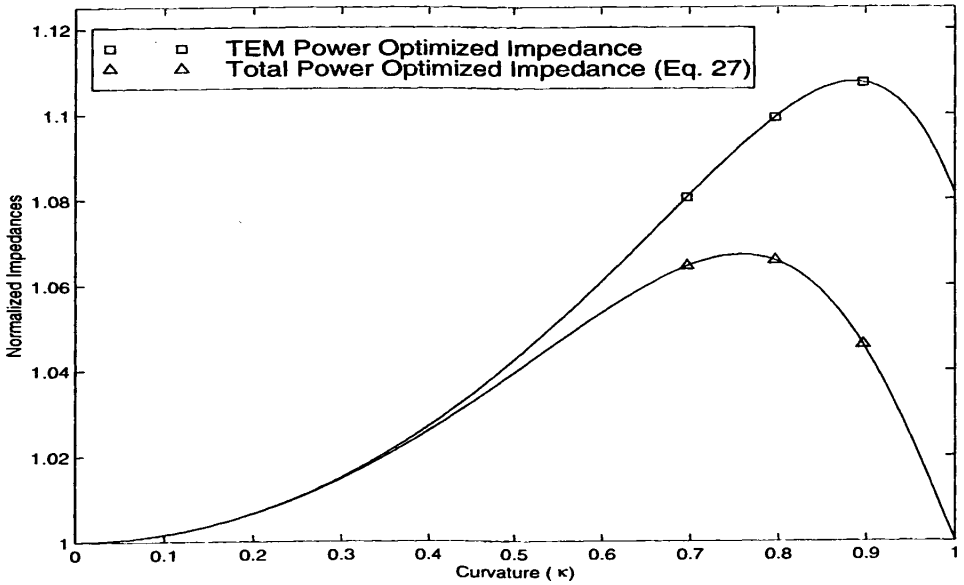

Figure 6: Normalized Optimum Impedances vs. Curvature

The value of the relative permittivity along the centerline of the bend that is required to generate these optimum impedances is proportional to the inverse of the square of the normalized impedances. Figure 7 shows the optimum relative permittivity curves as a function of curvature, normalized to the relative permittivity in the straight segments.

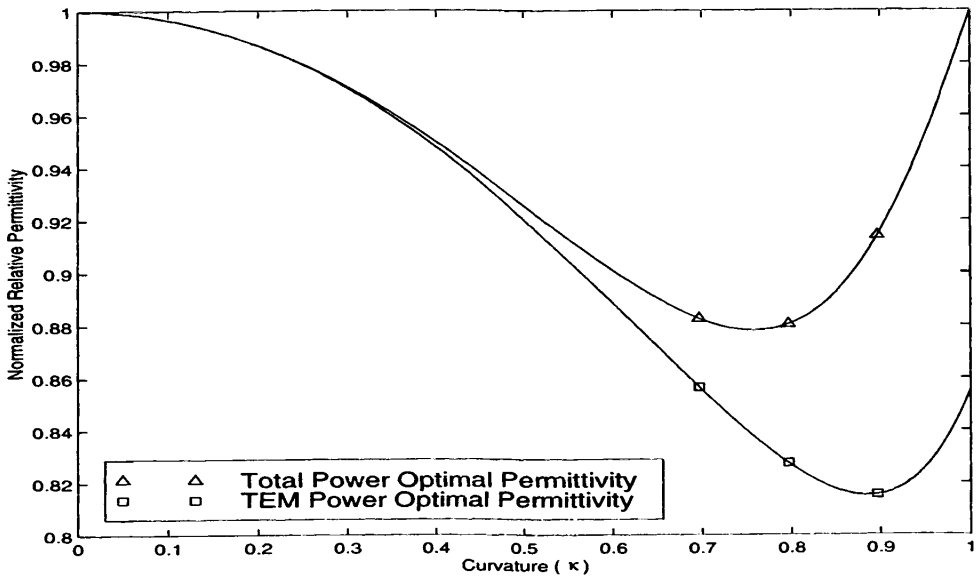

Figure 7: Optimum Relative Permittivities

4.1. TOTAL POWER RATIOS USING BOTH OPTIMIZING IMPEDANCES

The baseline ratios of optimized total transmitted power to "matched" total transmitted power using each of the two optimized impedances are plotted in Figure 8. As expected, using the impedance specifically optimized for total power provides a larger improvement in transmitted power compared to the matched case than using the impedance optimized for TEM power. Surprisingly, the 6-12% difference between the optimized and "matched" impedance values (see Figure 6) resulted in less than a 0.2% increase in optimized total transmitted power over matched total transmitted power. Also, for large curvature bends ($\kappa > 0.87$), the TEM optimized impedance actually transmits less total power than the "matched" impedance. The largest gain occurs at $\kappa = 0.74$, where the percentage of input power transmitted through the bend increased from 89.12% (matched) to 89.26% (optimized); a 0.14% increase in total power transmission and a 0.16% improvement over the matched impedance's performance.

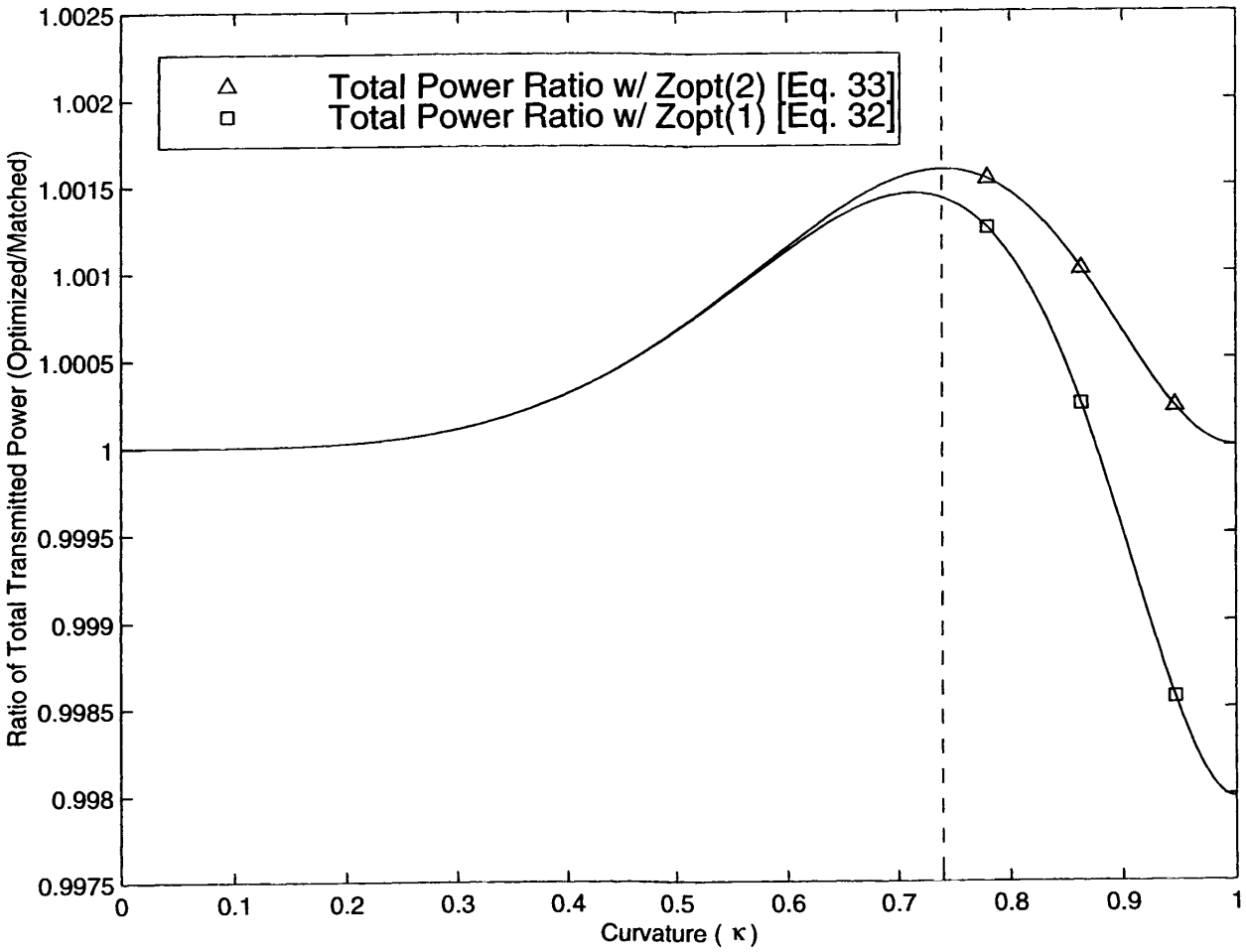

Figure 8: Ratios of Optimized Total Transmitted Power to Matched Total Transmitted Power

4.2. TEM POWER RATIOS USING BOTH OPTIMIZING IMPEDANCES

The baseline ratios of optimized TEM transmitted power to "matched" TEM transmitted power using each of the two optimized impedances are plotted in Figure 9. As expected, using the impedance specifically optimized for TEM power provides a larger improvement in transmitted power compared to the matched case than using the impedance optimized for total power. Again, despite the large difference in optimized and matched impedance values, the optimized TEM transmitted power was never more than 0.4% higher than the TEM power transmitted by the "matched" impedance. The largest gain occurs at $\kappa = 0.87$, where the percentage of input power transmitted through the bend and still in the TEM mode increased from 82.52% (matched) to 82.85% (optimized); a 0.33% increase in TEM power transmission and a 0.40% improvement over the matched impedance's performance.

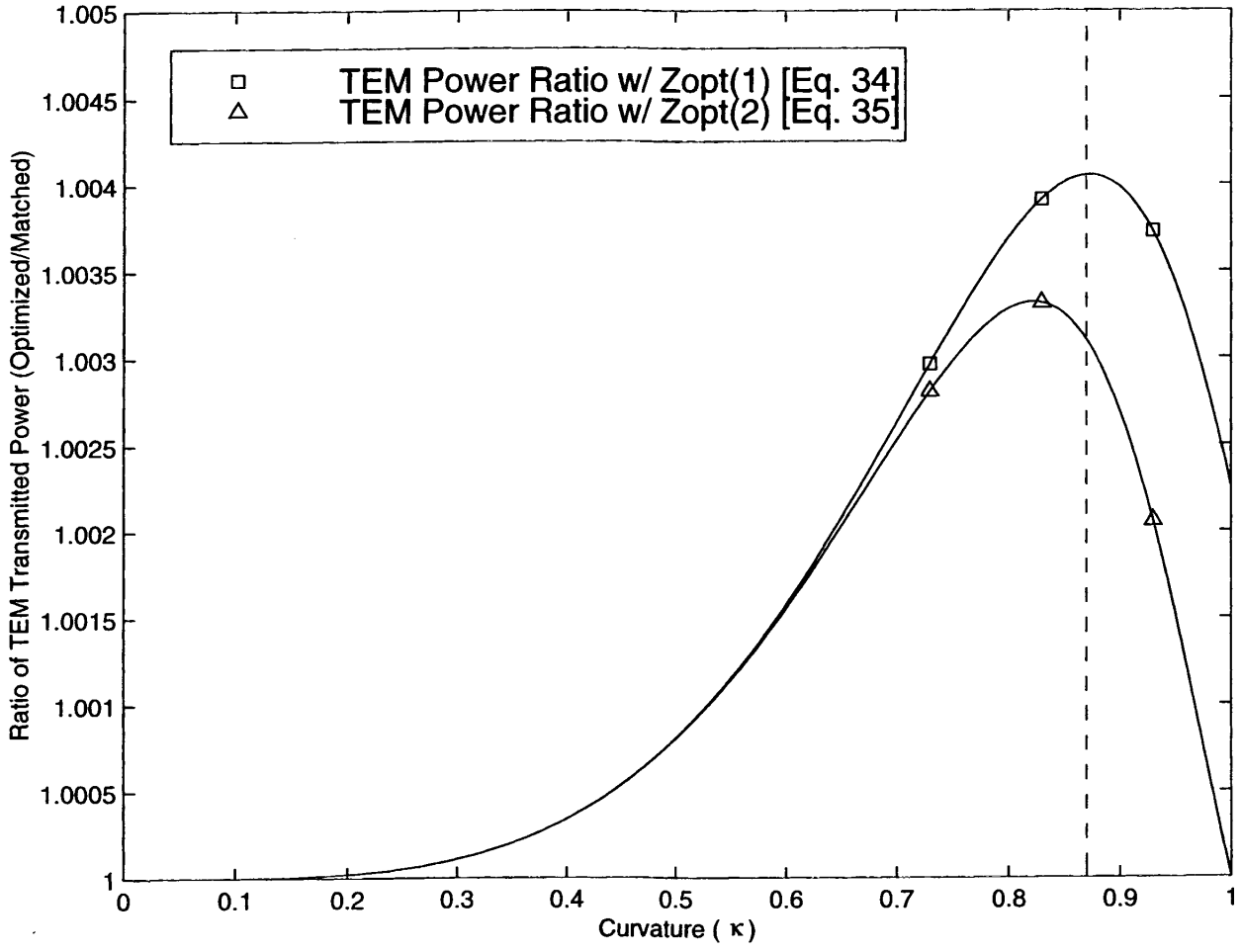

Figure 9: Ratios of Optimized TEM Transmitted Power to Matched TEM Transmitted Power

4.3. POWER FRACTION RATIOS USING BOTH OPTIMIZING IMPEDANCES

Finally, the baseline ratios of the optimized transmitted power fraction (TEM/Total power transmitted) to the "matched" transmitted power fraction for each of the two optimized impedances are shown in Figure 10. The optimized impedances will, at best, increase the fraction of the total power in the TEM mode by 0.5% over the matched impedance. The largest gain occurs at $\kappa = 0.95$, where the impedance used to optimize TEM transmission improves the power fraction from 96.19% (matched) to 96.67% (optimized); a 0.48% increase in the fraction of total power transmitted in the TEM mode and a 0.50% improvement over the matched impedance's performance.

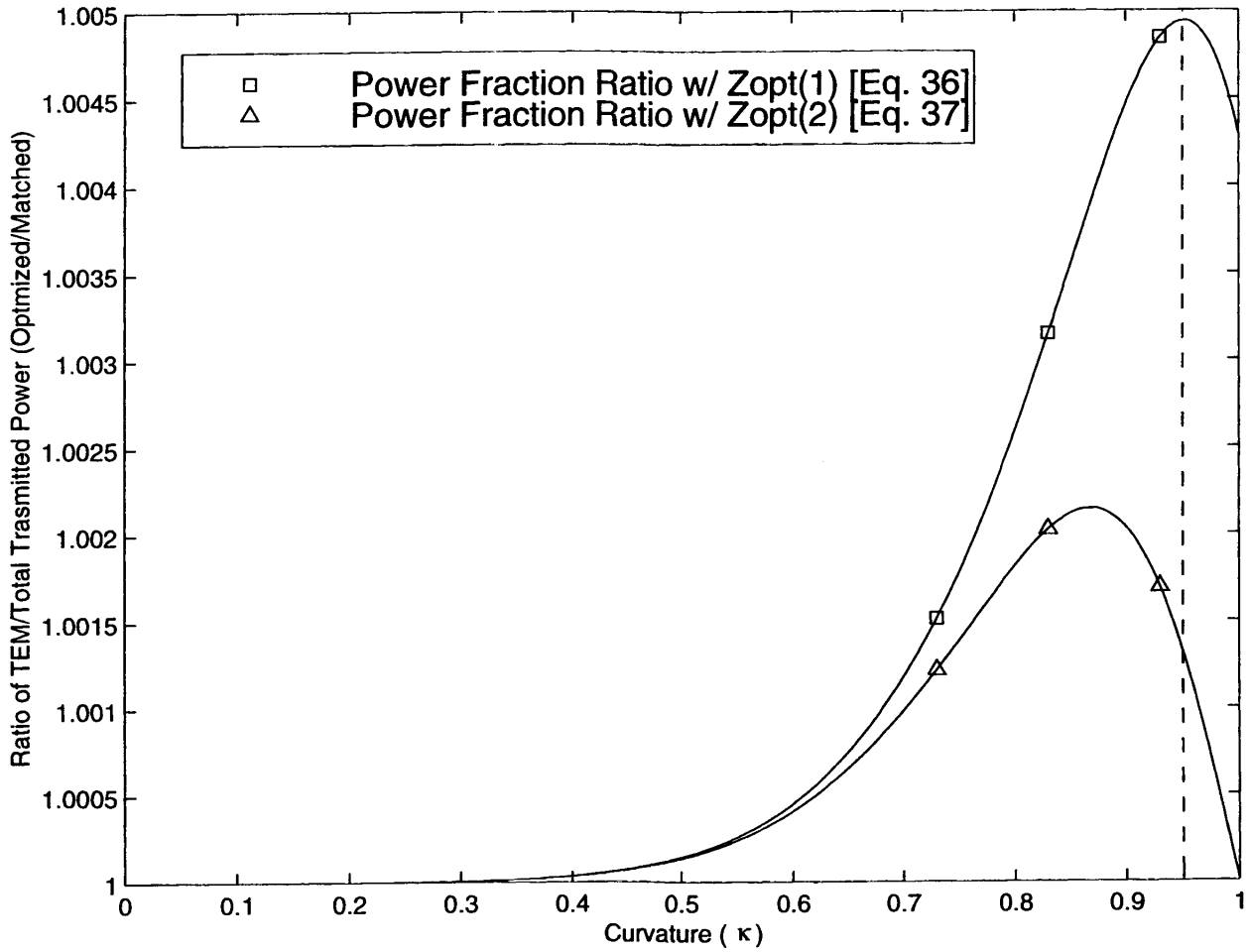

Figure 10: Ratios of Optimized Power Fractions to Matched Power Fractions (TEM/Total Power)

5. CONCLUSIONS

The fraction of input power transmitted through a waveguide bend filled with a graded dielectric material is strongly dependent on curvature. An initial "gut feel" suggested matching the centerline value of the graded dielectric to the dielectric value of the adjoining waveguide segments, but analysis shows that the permittivity required to maximize power transmission could vary from this value by over 12%. However, additional calculations demonstrated that improvements in transmitted power using this optimized permittivity were nearly negligible. Furthermore, the largest increases are only achievable in very large curvature bends, which require material with a permittivity that can be varied over an extreme range of values to avoid dispersion. Thus, while matching the centerline value in the bend to the dielectric of the straight segments is not mathematically optimum, the results are close enough to consider it a first order "rule of thumb," especially for small curvature bends.

It should also be remembered that this analysis was based on a continuously graded dielectric material in the bend. Any attempt to build a similar device using radial layers of constant dielectric material would have lower transmission-coefficient values and would introduce dispersion. This analysis can be applied to calculate theoretical upper limits of transmission performance capability for layered waveguide bends.

APPENDIX A. Matching Guide Impedance for Improved Low Frequency Performance

This appendix reviews the results obtained after attempting to match the guide impedance within the bend to the guide impedance in the input and output waveguide segments. Assuming an incident TEM wave, the electric and magnetic fields in the input guide segment are constant. Therefore, the voltage and current found by integrating the fields are simply the field magnitudes scaled by the waveguide dimensions. Thus, the guide impedances for the E-plane and H-plane oriented input segments corresponding to Figure 2 are calculated in (A.1) and (A.2) below.

E-plane:

$$V = 2bE_i \quad \text{and} \quad I = aH_i \quad \text{so} \quad Z_g = \frac{V}{I} = \frac{2bE_i}{aH_i} = \frac{2b}{a} Z_i \tag{A.1}$$

H-plane:

$$V = aE_i \quad \text{and} \quad I = 2bH_i \quad \text{so} \quad Z_g = \frac{V}{I} = \frac{aE_i}{2bH_i} = \frac{a}{2b} Z_i \tag{A.2}$$

For the E-plane bend, the magnitude of the electric and magnetic fields just inside the first boundary are found using the intrinsic impedance defined in equation (2) and using the boundary ratio derived in equation (6).

$$E_B = \frac{2\Psi Z_{ref} E_i}{\Psi Z_{ref} + \Psi_{ref} Z_i} \tag{A.3}$$

$$H_B = \frac{2\Psi_{ref} E_i}{\Psi Z_{ref} + \Psi_{ref} Z_i} \tag{A.4}$$

The voltage is derived by integrating the electric field with respect to the radial variable, Ψ,

$$V = \int_{\Psi_{ref}-b}^{\Psi_{ref}+b} \frac{2\Psi Z_{ref} E_i}{\Psi Z_{ref} + \Psi_{ref} Z_i} d\Psi = 2E_i \int_{\Psi_{ref}-b}^{\Psi_{ref}+b} \frac{\Psi Z_{ref}}{\Psi Z_{ref} + \Psi_{ref} Z_i} d\Psi = 2E_i \Gamma_1 \tag{A.5}$$

where the integral is momentarily abbreviated as Γ_1.

$$\Gamma_1 \equiv \int_{\Psi_{ref}-b}^{\Psi_{ref}+b} \frac{\Psi Z_{ref}}{\Psi Z_{ref} + \Psi_{ref} Z_i} d\Psi \tag{A.6}$$

The current is derived by integrating the magnetic field with respect to the transverse variable, z. However, since the expression in (A.4) is independent of z, the result is simple scaling as in (A.1) above.

$$I = \frac{2a\Psi_{ref} E_i}{\Psi Z_{ref} + \Psi_{ref} Z_i} \tag{A.7}$$

But since this current is still a function of Ψ, the average current was derived,

$$I_{avg} = \frac{1}{2b}\int_{\Psi_{ref}-b}^{\Psi_{ref}+b} I\, d\Psi = \frac{a\Psi_{ref}E_i}{b}\int_{\Psi_{ref}-b}^{\Psi_{ref}+b} \frac{d\Psi}{\Psi Z_{ref} + \Psi_{ref} Z_i} = \frac{a\Psi_{ref}E_i}{b}\Gamma_2 \tag{A.8}$$

where the integral is momentarily abbreviated as Γ_2.

$$\Gamma_2 \equiv \int_{\Psi_{ref}-b}^{\Psi_{ref}+b} \frac{d\Psi}{\Psi Z_{ref} + \Psi_{ref} Z_i} \tag{A.9}$$

Thus, the E-plane guide impedance is found from (A.5) and (A.8) as

$$Z_g = \frac{V}{I_{avg}} = \frac{2b\Gamma_1}{a\Psi_{ref}\Gamma_2}. \tag{A.10}$$

For the H-plane bend, the expressions for the magnitude of the electric and magnetic fields just inside the first boundary are the same as for the E-plane, given in (A.3) and (A.4) above, but the fields are oriented differently. The voltage is derived by integrating the electric field with respect to the transverse variable, z, resulting in the scaled expression below.

$$V = \frac{2a\Psi Z_{ref} E_i}{\Psi Z_{ref} + \Psi_{ref} Z_i} \tag{A.11}$$

Since this voltage is still a function of Ψ, the average voltage was derived.

$$V_{avg} = \frac{1}{2b}\int_{\Psi_{ref}-b}^{\Psi_{ref}+b} V d\Psi = \frac{aE_i}{b}\int_{\Psi_{ref}-b}^{\Psi_{ref}+b} \frac{\Psi Z_{ref}}{\Psi Z_{ref} + \Psi_{ref} Z_i} d\Psi = \frac{aE_i}{b}\Gamma_1 \tag{A.12}$$

The current is derived by integrating the magnetic field with respect to the radial variable, Ψ.

$$I = \int_{\Psi_{ref}-b}^{\Psi_{ref}+b} \frac{2\Psi_{ref}E_i}{\Psi Z_{ref} + \Psi_{ref} Z_i} d\Psi = 2\Psi_{ref}E_i \int_{\Psi_{ref}-b}^{\Psi_{ref}+b} \frac{d\Psi}{\Psi Z_{ref} + \Psi_{ref} Z_i} = 2\Psi_{ref}E_i\Gamma_2 \tag{A.13}$$

Thus, the H-plane guide impedance is found from (A.12) and (A.13) as

$$Z_g = \frac{V_{avg}}{I} = \frac{a\Gamma_1}{2b\Psi_{ref}\Gamma_2} \tag{A.14}$$

Comparing the guide impedance expressions in (A.1) and (A.2) with (A.10) and (A.14), respectively, the guide impedances for both the E-plane and H-plane cases will be matched if we can enforce the expression in (A.15).

$$Z_i = \frac{\Gamma_1}{\Psi_{ref}\Gamma_2} \qquad \text{or} \qquad \Gamma_1 = \Psi_{ref} Z_i \Gamma_2 \tag{A.15}$$

Expanding the first integral, given in (A.6), we discover

$$\Gamma_1 = \int_{\Psi_{ref}-b}^{\Psi_{ref}+b} \left[1 - \frac{\Psi_{ref} Z_i}{\Psi Z_{ref} + \Psi_{ref} Z_i}\right] d\Psi = 2b - \Psi_{ref} Z_i \int_{\Psi_{ref}-b}^{\Psi_{ref}+b} \frac{d\Psi}{\Psi Z_{ref} + \Psi_{ref} Z_i}$$

$$\Gamma_1 = 2b - \Psi_{ref} Z_i \Gamma_2 . \tag{A.16}$$

Combining (A.15) and (A.16) requires

$$\Gamma_2 = \frac{b}{\Psi_{ref} Z_i} = \frac{\kappa}{Z_i} \tag{A.17}$$

where $\kappa = \dfrac{b}{\Psi_{ref}}$.

Finally, evaluating (A.9) produces

$$\Gamma_2 = \int_{\Psi_{ref}-b}^{\Psi_{ref}+b} \frac{d\Psi}{\Psi Z_{ref} + \Psi_{ref} Z_i} = \frac{1}{Z_{ref}} \left[\ln(\Psi Z_{ref} + \Psi_{ref} Z_i)\right]_{\Psi_{ref}-b}^{\Psi_{ref}+b}$$

$$= \frac{1}{Z_{ref}} \left[\frac{\ln((\Psi_{ref}+b)Z_{ref} + \Psi_{ref} Z_i)}{\ln((\Psi_{ref}-b)Z_{ref} + \Psi_{ref} Z_i)}\right] = \frac{1}{Z_{ref}} \left[\frac{\ln((1+\kappa)Z_{ref} + Z_i)}{\ln((1-\kappa)Z_{ref} + Z_i)}\right] \tag{A.18}$$

Thus, to guarantee the guide impedances are matched across the boundaries, we must determine Z_{ref} as a function of Z_i and κ by solving the following expression.

$$\frac{\kappa}{Z_i} = \frac{1}{Z_{ref}} \left[\frac{\ln((1+\kappa)Z_{ref} + Z_i)}{\ln((1-\kappa)Z_{ref} + Z_i)}\right] \tag{A.19}$$

Or, more simply, by defining the ratio of the impedances to be $\gamma = \dfrac{Z_i}{Z_{ref}}$,

$$\kappa = \gamma \left[\frac{\ln(1+\gamma+\kappa)}{\ln(1+\gamma-\kappa)}\right]. \tag{A.20}$$

Solving (A.20) numerically to determine γ for all possible values of κ and then inverting to get an expression for Z_{ref} normalized by Z_i produces the data in the plot below and compared to the two impedances derived earlier for optimizing power transmission.

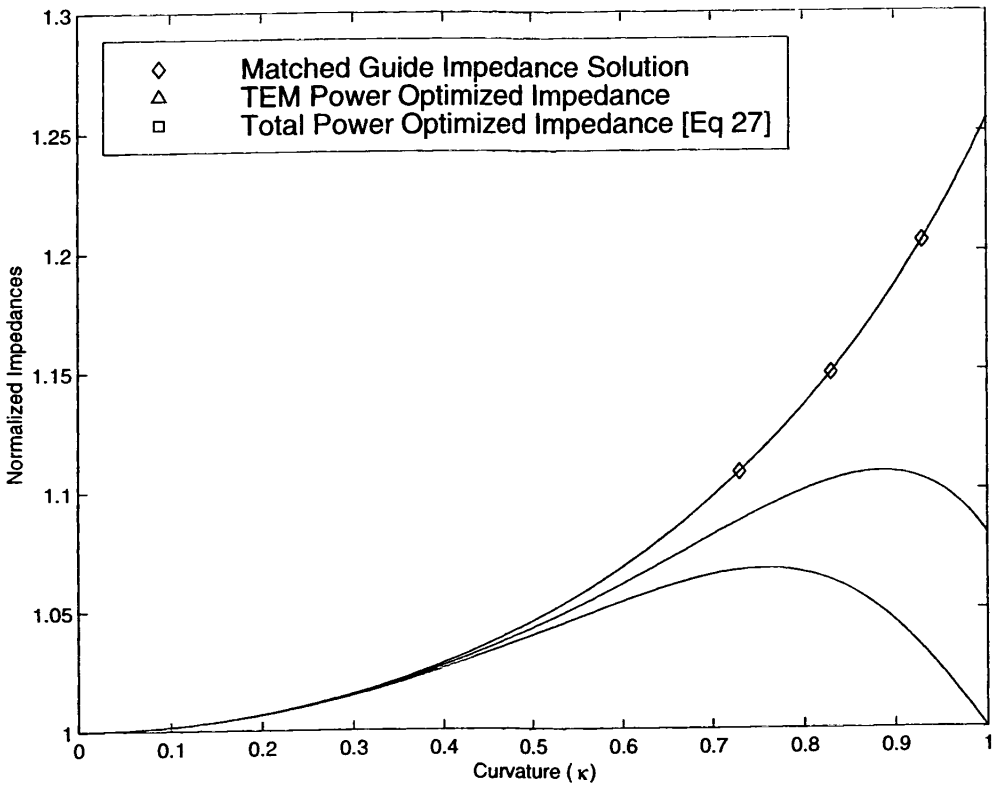

Figure A1: Normalized Impedance Comparison vs. Curvature

As expected, the impedances are very similar for low curvature bends, and asymptotically approach unity as curvature goes to zero. The quick and increasing divergence with increasing values of κ was surprising, however.

Since the "rule of thumb" derived earlier was to "match" the centerline impedance to the input waveguide ($Z_{ref} = Z_i$), a comparison of these two impedance choices was also generated. Figure A2, below, compares the total power transmitted through the bend using the guide impedance solution with the total power transmitted by the constant "matched" impedance value. The results are very similar, so Figure A3 shows the ratio of the two plots in Figure 2A. The matched guide impedance outperforming the "matched" impedance by a negligible amount for medium curvature values (less than 0.5%), then drops off quickly for large curvature bends, but the transmitted power of the two solutions never differ by more than 2% for any value of κ.

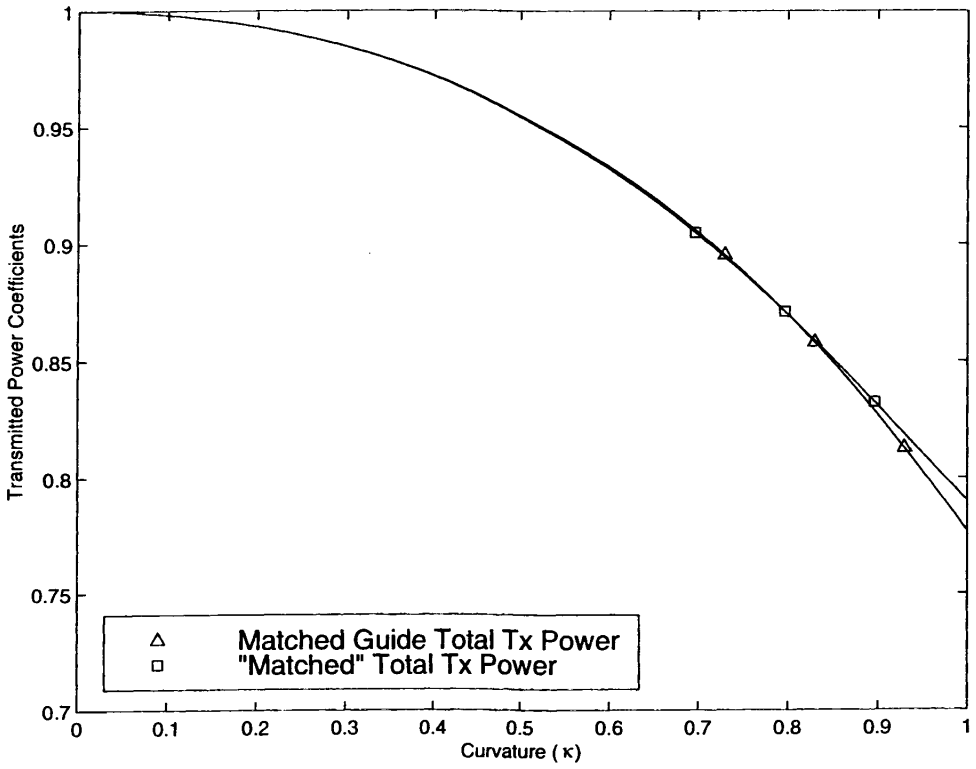

Figure A2: Power Coefficients for "Matched" Impedance and Matched Guide Impedance

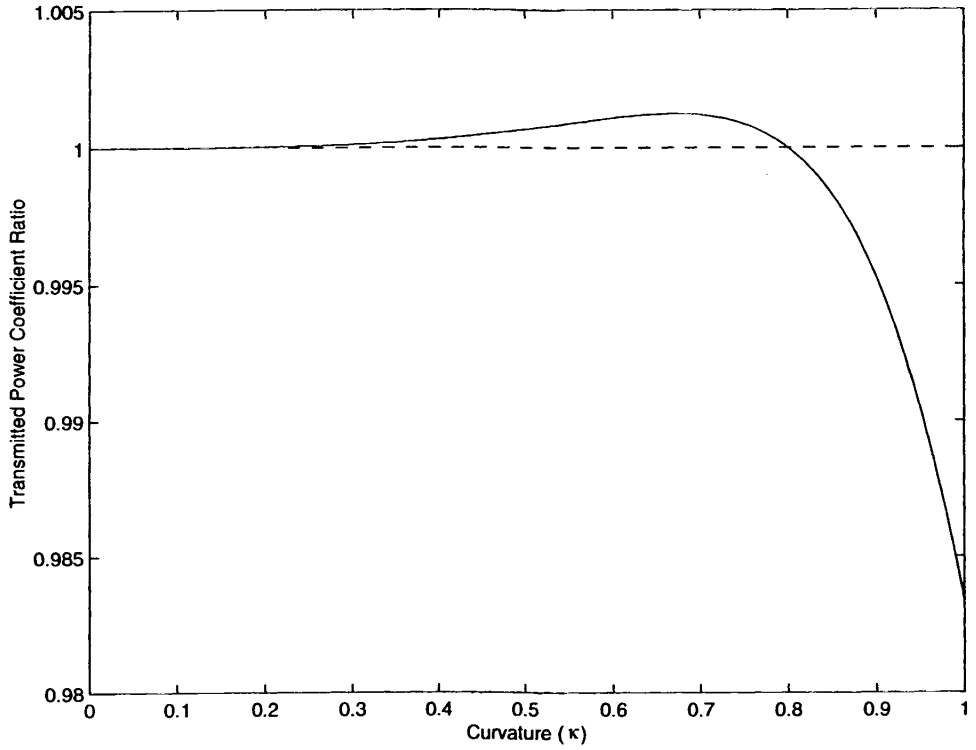

Figure A3: Ratio of Coefficients for "Matched" Impedance and Matched Guide Impedance

APPENDIX B. Different Incident and Transmitted Region Impedances

This appendix briefly reviews the results obtained after modifying some of the equations previously derived to reflect the situation when the impedances in the straight segments connected to the bend are not equal. The transmission ratio at the first boundary, given in equation (6), is updated by replacing Z_i with Z_I, while the transmission ratio at the second boundary, given in equation (7), is updated by replacing Z_i with Z_T. The total transmission ratio, previously expressed in equation (8), would be transformed into (B.1) below.

$$\frac{E_T}{E_I} = \frac{4\Psi\Psi_{ref}Z_{ref}Z_T}{(\Psi Z_{ref} + \Psi_{ref}Z_I)(\Psi Z_{ref} + \Psi_{ref}Z_T)} \tag{B.1}$$

Following the same procedure through equations (9) and (10), the average value of the transmitted electric field can then be derived.

$$E_{TEM} = \frac{(E_T)_{avg}}{E_I} = \frac{2Z_T}{\kappa(Z_I - Z_T)Z_{ref}}\left[Z_I \ln\left(\frac{(1+\kappa)Z_{ref} + Z_I}{(1-\kappa)Z_{ref} + Z_I}\right) - Z_T \ln\left(\frac{(1+\kappa)Z_{ref} + Z_T}{(1-\kappa)Z_{ref} + Z_T}\right)\right] \tag{B.2}$$

where $\kappa = b/\Psi_{ref}$.

The incident power becomes

$$P_I = \int_0^a \int_{\Psi_{ref}-b}^{\Psi_{ref}+b} \left|\overline{E}_I \times \overline{H}_I\right| d\Psi\, dz = \frac{E_I^2}{Z_I}(2ab), \tag{B.3}$$

and the total transmitted power developed in (12) and (13) are shown modified below.

$$P_{TOT} = \int_0^a \int_{\Psi_{ref}-b}^{\Psi_{ref}+b} \left|\overline{E}_T \times \overline{H}_T\right| d\Psi\, dz = \frac{E_I^2}{Z_T}\int_0^a \int_{\Psi_{ref}-b}^{\Psi_{ref}+b} \left(\frac{E_T}{E_I}\right)^2 d\Psi\, dz \tag{B.4}$$

$$P_{TOT} = \frac{32abZ_TE_I^2}{\kappa Z_{ref}(Z_I - Z_T)^3}\left[Z_IZ_T \ln\left(\frac{(1-\kappa^2)Z_{ref}^2 + (1-\kappa)Z_IZ_{ref} + (1+\kappa)Z_TZ_{ref} + Z_IZ_T}{(1-\kappa^2)Z_{ref}^2 + (1+\kappa)Z_IZ_{ref} + (1-\kappa)Z_TZ_{ref} + Z_IZ_T}\right) + \kappa Z_{ref}(Z_I - Z_T)\left(\frac{Z_I^2}{(1-\kappa^2)Z_{ref}^2 + 2Z_IZ_{ref} + Z_I^2} + \frac{Z_T^2}{(1-\kappa^2)Z_{ref}^2 + 2Z_TZ_{ref} + Z_T^2}\right)\right] \tag{B.5}$$

The transmitted power in the TEM mode is

$$P_{TEM} = \int_0^a \int_{\Psi_{ref}-b}^{\Psi_{ref}+b} \left| \bar{E}_{TEM} \times \bar{H}_{TEM} \right| d\Psi\, dz = \frac{(E_T)_{avg}^2}{Z_T}(2ab). \tag{B.6}$$

Thus, the transmitted power coefficients given in (15) and (16) become (B.7) and (B.8).

$$T_{TOT} = \frac{P_{TOT}}{P_i} = \frac{16 Z_I Z_T}{\kappa Z_{ref} (Z_I - Z_T)^3} \left[\begin{array}{l} Z_I Z_T \ln\left(\dfrac{(1-\kappa^2) Z_{ref}^2 + (1-\kappa) Z_I Z_{ref} + (1+\kappa) Z_T Z_{ref} + Z_I Z_T}{(1-\kappa^2) Z_{ref}^2 + (1+\kappa) Z_I Z_{ref} + (1-\kappa) Z_T Z_{ref} + Z_I Z_T} \right) \\ + \kappa Z_{ref} (Z_I - Z_T) \left(\dfrac{Z_I^2}{(1-\kappa^2) Z_{ref}^2 + 2 Z_I Z_{ref} + Z_I^2} + \dfrac{Z_T^2}{(1-\kappa^2) Z_{ref}^2 + 2 Z_T Z_{ref} + Z_T^2} \right) \end{array} \right] \tag{B.7}$$

$$\begin{aligned} T_{TEM} &= \frac{P_{TEM}}{P_I} = \left(\frac{(E_T)_{avg}^2 / Z_T}{E_I^2 / Z_I} \right) = \frac{Z_I}{Z_T} \left(\frac{(E_T)_{avg}}{E_I} \right)^2 = \frac{Z_I}{Z_T} E_{TEM}^2 \\ &= \frac{4 Z_I Z_T}{\kappa^2 (Z_I - Z_T)^2 Z_{ref}^2} \left[Z_I \ln\left(\frac{(1+\kappa) Z_{ref} + Z_I}{(1-\kappa) Z_{ref} + Z_I} \right) - Z_T \ln\left(\frac{(1+\kappa) Z_{ref} + Z_T}{(1-\kappa) Z_{ref} + Z_T} \right) \right]^2 \end{aligned} \tag{B.8}$$

Equations (B.7) and (B.8) were numerically analyzed using MatLab® to determine the values of Z_{ref} that will maximize the transmission coefficients, resulting in two optimized impedance curves as a function of curvature. When these curves were normalized with respect to the geometrical average of the two straight segment impedances, $\sqrt{Z_I Z_T}$, the results were nearly identical to the normalized optimization curves found and shown in Figure 6.

Thus, in the more generalized case where the input and output impedances attached to a bend with a relatively low curvature do not have matching impedances, the power transmission can be maximized by setting $Z_{ref} = \sqrt{Z_I Z_T}$. Similarly, for bends with larger curvature values, this impedance value can be optimized using equations (24 or 27-31) or the curves in Figure 6, but the resulting power improvement will be negligible. In either case, the theoretical maximum transmitted power will be reduced for the case with different straight segment impedances compared to the special case when the impedances are equal.

REFERENCES

1. C. E. Baum, *Two-Dimensional Inhomogeneous Dielectric Lenses for E-Plane Bends of TEM Waves Guided Between Perfectly Conducting Sheets*, Sensor and Simulation Note 388, October 1995.

2. C. E. Baum, *Use of Generalized Inhomogeneous TEM Plane Waves in Differential Geometric Lens Synthesis*, Sensor and Simulation Note 405, December 1996.

3. C. E. Baum, *Dielectric Body-of-Revolution Lenses with Azimuthal Propagation*, Sensor and Simulation Note 393, March 1996.

4. C. E. Baum, J. J. Sadler and A. P. Stone, *A Prolate Spheroid Uniform Isotropic Dielectric Lens Feeding a Circular Coax*, Sensor and Simulation Note 335, December 1991.

5. C. E. Baum, *Some Features of Waveguide/Horn Design*, Sensor and Simulation Note 314, November 1988.

6. C. E. Baum, *Admittance of Bent TEM Waveguides in a CID Medium*, Sensor and Simulation Note 436, May 1999.